Metabolism Clinical and Experimental 101 (2019) 153999

Contents lists available at ScienceDirect

Metabolism Clinical and Experimental

journal homepage: www.metabolismjournal.com

The Rho GTPase RND3 regulates adipocyte lipolysis

Simon N. Dankel [a,b,*], Therese H. Røst [a,b], Agné Kulyté [c], Zina Fandalyuk [a], Thomas Skurk [d,e], Hans Hauner [e,f], Jørn V. Sagen [a,b], Mikael Rydén [c], Peter Arner [c], Gunnar Mellgren [a,b,*]

[a] Mohn Nutrition Research Laboratory, Department of Clinical Science, University of Bergen, N-5020 Bergen, Norway
[b] Hormone Laboratory, Haukeland University Hospital, N-5021 Bergen, Norway
[c] Department of Medicine (H7), Karolinska Institutet, C2-94 Karolinska University Hospital, Huddinge, 141 86 Stockholm, Sweden
[d] ZIEL Institute for Food and Health, Technical University of Munich, 85354 Freising, Germany
[e] Else Kroener-Fresenius Centre for Nutritional Medicine, School of Medicine, Technical University of Munich, 80992 Munich, Germany
[f] German Center of Diabetes Research, Helmholtz Center, Munich, Germany

ARTICLE INFO

Article history:
Received 18 July 2019
Accepted 23 October 2019

Keywords:
Adipose tissue
Adipocyte
Metabolism
Obesity
Insulin resistance
Inflammation

ABSTRACT

Background: Adipose tissue plays a crucial role in diet- and obesity-related insulin resistance, with implications for several metabolic diseases. Identification of novel target genes and mechanisms that regulate adipocyte function could lead to improved treatment strategies. RND3 (RhoE/Rho8), a Rho-related GTP-binding protein that inhibits Rho kinase (ROCK) signaling, has been linked to diverse diseases such as apoptotic cardiomyopathy, heart failure, cancer and type 2 diabetes, in part by regulating cytoskeleton dynamics and insulin-mediated glucose uptake.

Results: We here investigated the expression of *RND3* in adipose tissue in human obesity, and discovered a role for RND3 in regulating adipocyte metabolism. In cross-sectional and prospective studies, we observed 5-fold increased adipocyte levels of *RND3* mRNA in obesity, reduced levels after surgery-induced weight loss, and positive correlations of *RND3* mRNA with adipocyte size and surrogate measures of insulin resistance (HOMA2-IR and circulating triglyceride/high-density lipoprotein cholesterol (TAG/HDL-C) ratio). By screening for *RND3*-dependent gene expression following siRNA-mediated *RND3* knockdown in differentiating human adipocytes, we found downregulation of inflammatory genes and upregulation of genes related to adipocyte ipolysis and insulin signaling. Treatment of adipocytes with tumor necrosis factor alpha (TNFα), lipopolysaccharide (LPS), hypoxia or cAMP analogs increased *RND3* mRNA levels 1.5–2-fold. Functional assays in primary human adipocytes confirmed that *RND3* knockdown reduces cAMP- and isoproterenol-induced lipolysis, which were mimicked by treating cells with ROCK inhibitor. This effect could partly be explained by reduced protein expression of adipose triglyceride lipase (ATGL) and phosphorylated hormone-sensitive lipase (HSL).

Conclusion: We here uncovered a novel differential expression of adipose *RND3* in obesity and insulin resistance, which may at least partly depend on a causal effect of RND3 on adipocyte lipolysis.

1. Introduction

Obesity-related risk of morbidity and mortality [1] involves systemic insulin resistance linked to inflammation in adipose tissue [2,3], which may largely distinguish people with metabolically "unhealthy" and "healthy" obesity [4]. Increased adipose tissue inflammation further associates with elevated circulating free fatty acids (FFA), visceral and ectopic lipid accumulation and lipotoxicity, likely in large part due to increased adipocyte lipolysis [5–8]. Identification of novel genes and pathways that mediate altered adipose tissue function in obesity is therefore of great interest, and may enable development of new therapeutic strategies.

Lipolysis in adipocytes is critical for lipid handling and systemic metabolic homeostasis [9]. Adipocyte lipolysis increases during fasting, exercise and other factors to release FFA for use by other tissues and organs, in part induced by beta-adrenergic stimuli. These stimuli induce the cyclic adenosine monophosphate (cAMP)/protein kinase A (PKA) pathway, and consequently activate lipolytic enzymes, most notably hormone-sensitive lipase (HSL) by phosphorylating activity-

Abbreviations: AMPK, 5′ adenosine monophosphate-activated protein kinase; B6, C57BL/6 inbred mouse strain; BTBR, Black and Tan BRachyury mouse strain; cAMP, cyclic adenosine monophosphate; hASC, primary human adipose stromal cells; HOMA2-IR, homeostatic model assessment 2 of insulin resistance; HIF-1α/HIF1A, hypoxia-inducible factor-1α; HSL, hormone-sensitive lipase; Ob, obese; Ob/ob, obese leptin-deficient mice; OM, omental; PKA, protein kinase A; PPARγ, peroxisome proliferator-activated receptor gamma; RND3, Rho-related GTP-binding protein RhoE/Rho8; ROCK, Rho-associated, coiled-coil-containing protein kinase; SC, subcutaneous; SVF, stromal vascular fraction.

* Corresponding authors at: Department of Clinical Science, University of Bergen, Haukeland University Hospital, N-5021 Bergen, Norway.
E-mail addresses: simon.dankel@uib.no (S.N. Dankel), gunnar.mellgren@uib.no (G. Mellgren).

https://doi.org/10.1016/j.metabol.2019.153999

controlling serine residues (i.e., ser650, corresponding to ser651 in mouse and ser660 in rat) [10–12]. Additional pathways also stimulate lipolysis via HSL and/or other enzymes [13], such as activation of adipose triglyceride lipase (ATGL) by 5′ adenosine monophosphate-activated protein kinase (AMPK) [14]. Feeding and increased insulin levels inhibit these processes in a normal physiologic regulation [9]. However, while short-term overfeeding (for a few days) does not provoke dysregulated lipolysis in adipocytes [15], conditions of chronic nutrient stress over weeks and months may increase lipolysis in conjunction with developing insulin resistance in adipocytes. Hence, a partial reduction in lipolysis may enhance glucose metabolism [6]. Genetic evidence and different experimental models further support that genotype-dependent increases in lipolysis may cause insulin resistance and metabolic diseases by promoting visceral and ectopic fat accumulation [7,16], although de novo lipogenesis and impaired lipid handling in adipocytes may also contribute [17].

RND3 (Rho-related GTP-binding protein RhoE/Rho8) is a member of the Rnd family, which represents a sub-group of the Rho family of small GTP-binding proteins (G-proteins). The Rnd family also includes Rnd1 (Rho6) and Rnd2 (Rho7) [18]. Most small G-proteins are molecular switches, which cycle between a non-active, resting GDP-bound form and an active.

GTP-bound form [18]. However, unlike RND1 and RND2, RND3 with its unique structure [19] has no intrinsic GTPase activity and is insensitive to the Rho-specific GTPase-activating proteins (GAPs) [20]. Through its basic function in regulating the formation of actin stress fibers and cytoskeleton dynamics, RND3 has been implicated as a driving factor in the pathophysiology of diseases such as apoptotic cardiomyopathy, heart failure, and cancer [21]. RND3 acts in part by inhibiting the activity of RhoA and its downstream effector Rho-associated coiled-coil containing kinase 1 (ROCK1), signals that induce stress fiber formation [22]. RND3 was previously shown to impair insulin-mediated glucose uptake in skeletal muscle of patients with obesity and T2D through direct binding and inhibition of ROCK1 [23]. Furthermore, in gastric cancer cells, hypoxia-inducible factor-1α (HIF-1α), a transcription factor implicated in adipose tissue insulin resistance and inflammation [24,25], was found to bind a hypoxia-responsive element (HRE) in the *RND3* promoter to induce *RND3* expression [26]. These data point to a possible role for RND3 in regulating adipose tissue function. We here hypothesized that *RND3* regulates adipose tissue metabolism and function in humans, with a possible role in obesity and insulin resistance.

2. Methods

2.1. Ethics and Subjects

The study was approved by the Regional Ethics Committee (REK Vest, Norway, approval numbers 2010/512 and 2010/3405, and the Regional Committee of Ethics in Stockholm, Sweden). Each subject gave written informed consent. Blood and adipose tissue biopsies were collected from three cohorts (Cohorts 1–3, Table 1).

2.2. Adipose Tissue Sampling

Human adipose tissue was analyzed for three different cohorts. Subcutaneous (SC) and omental (OM) adipose tissue biopsies were obtained by surgical excision from patients with severe obesity undergoing bariatric surgery in Western Norway (Førde Hospital and Voss Hospital), as previously described [27,28] (Cohorts 1–2, Table 1). Subcutaneous biopsies were also obtained from a subset of patients one year after bariatric surgery and from non-obese healthy people (Cohort 1) [27]. In Cohort 2 [28], adipocytes and the stromal vascular fraction (SVF) were isolated from SC adipose tissue. In Cohort 3 [29], subcutaneous adipose tissue samples were collected by needle biopsy from the periumbilical region of non-obese ($n = 26$) and obese ($n = 30$) women. Clinical details of Cohort 3 as well as sample preparation and gene microarrays are described in the original publication [29]. The samples were collected between 2003 and 2010.

2.3. Adipose Tissue Homogenization and Fractionation

Frozen whole tissue (200-300 mg) was homogenized in a 2 mL safe-lock eppendorf tube with 1 mL Qiazol lysing buffer (Qiagen) and a 5 mm metal bead (Millipore), using a TissueLyser (Qiagen) with three repeated shakings at 25 Hz for 2 min each. To isolate adipocytes and SVF, 700–800 mg of adipose tissue was treated with collagenase and thermolysin (Liberase Blendzyme 3, Roche), and completed within 1 h ±5 min, as previously described [30]. The tissue/cells were frozen immediately and stored at −80°C for later gene expression analysis.

2.4. Adipocyte Cultures

Primary human adipose stromal cells (hASCs) were isolated from subcutaneous liposuction aspirate, cultured and differentiated, as described previously [30]. 3T3-L1 cells were cultured in 24-wells plates in DMEM 4.5 g/L glucose containing 1% penicillin and streptomycin (PEST), at 37°C, as described previously [31]. For the hypoxia experiment, the adipocytes were placed in an incubator with an atmosphere of 2% oxygen, 5% CO2 and 93% N2, to be compared with the standard atmosphere (5% CO2, 21% oxygen and 74% N2). Human preadipocytes from the human SGBS adipocyte cell line [32] were cultured and propagated in proliferation medium consisting of DMEM-Ham's F-12 (1:1) supplemented with 10% fetal calf serum (FCS), 33 μM biotin, 20 μM DL-pantothenate, 100 U/mL penicillin and 100 μg/ml streptomycin. Differentiation was induced with DMEM/F12 medium containing 10 μg/mL transferrin, 66 nM insulin, 1 nM triiodothyronine (T3) and 100 nM cortisol. During the first 4 days of differentiation, the medium was also

Table 1
Overview of cohorts and clinical data.

	M/F	Age (years)	BMI (kg/m^2)	HOMA2-IR	TAG/HDL	Figure
Cohort 1						
Lean	7/6	44.0 ± 17.5	23.0 ± 2.5	1.45 ± 0.63[a]	0.83 ± 0.45	1B
Obese	4/12	39.4 ± 10.9	53.3 ± 4.3	3.0 ± 1.65	1.48 ± 0.74	
Post-surgery	4/12	40.3 ± 10.9	33.1 ± 5.0	1.63 ± 0.64	1.50 ± 1.18	
Cohort 2						
Lean	5/7	43.5 ± 11.6	22.8 ± 2.1	1.11 ± 0.40	0.96 ± 0.67	1C-D, 2A
Obese	4/8	43.2 ± 9.98	43.7 ± 5.2	2.38 ± 1.00	2.36 ± 1.09	
Post-surgery	1/5	43.8 ± 9.13	32.9 ± 5.7	1.32 ± 0.38	0.95 ± 0.36	
Cohort 3						
Non-obese/obese	0/56	42.9 ± 12.0	33.1 ± 9.9	1.38 ± 1.15	N/A	2B

M/F, male/female; BMI, body-mass index (kg/m^2); OM, omental adipose tissue; Pre, before bariatric surgery; Post-surgery, one year after bariatric surgery/after profound fat loss; HOMA2-IR, homeostatic model assessment 2 of insulin resistance; TAG, triacylglycerol; HDL, high-density lipoprotein cholesterol.
[a] $n = 6$ due to missing data.

supplemented with 500 μM 3-isobutyl-1-methylxanthine, 25 nM dexamethasone and 2 μM rosiglitazone. For some experiments, cells were treated with the cAMP analogs 8CPT-cAMP or dibutyryl cAMP (dcAMP) (activators of PKA as well as Exchange protein activated by cAMP (Epac) signaling), 6 MB-cAMP (activator of PKA signaling), isoproterenol (β3-adrenergic receptor agonist) or ROCK inhibitor (Y27632, selective inhibitor of p160ROCK).

2.5. siRNA Transfection

After differentiation for up to 11 days, hASCs were transfected for 48-72 h with 25 nM ON-TARGETplus human siRNA SMARTpool (Dharmacon, Thermo Fisher Scientific) using HiPerFect (Qiagen) (non-targeting siRNA control and siRNA against RND3 (L-007794-00-0005) or HIF1A (J-004018-07). Cells were collected in buffer RLT (Qiagen) and stored at −80°C until RNA extraction.

For the lipolysis assay (see below), hASCs were transfected at day 8 of differentiation with siRNAs targeting RND3 or a scramble non-targeting siRNA pool using Neon electroporator (Invitrogen) according to the manufacturer's protocol. Briefly, for one transfection reaction 1 million of hASCs suspended in 90 μL of R buffer were mixed with 200 pmol/μL of siRNA and transfection was performed using a 100 μL electroporation tip. Electroporation conditions were 1400 Volts, 20 ms width, and 2 pulses. Following electroporation the cells were plated in 48-well plates at a density of 55.000 cells/well in 250 μL medium, with a final siRNA concentration of 40 nM. The next day medium was replaced to the fresh medium with reduced insulin (0.01 nM), and ROCK inhibitor was added at a final concentration of 10 μM, followed by incubation of the cells for 72 h. Each sample was prepared in quadruplicates and the experiment was repeated three times.

2.6. RNA Extraction

The RNeasy Lipid Tissue Midi Kit (whole tissue) or Mini Kit (Qiagen) was used to extract total RNA. NanoDrop spectrophotometer and Agilent 2100 Bioanalyzer were used to measure amount (ng/μL) and quality (RNA integrity number) of RNA.

2.7. qPCR Analysis

cDNA was prepared from 1 μg total RNA by the Transcriptor First Strand cDNA Synthesis Kit (Roche), and diluted 1:10 with PCR-grade water. For the cell fractions and cell culture, the SuperScript® VILO™ cDNA Synthesis Kit (Invitrogen) was used, with an input of 100 ng (cell fractions) and 500 ng (cell culture) total RNA per sample, followed by 1:20 dilution with PCR-grade water. The LightCycler480 Probes Master kit and the LightCycler480 rapid thermal cycler system (Roche Applied Science) were used to perform qPCR. Target and reference genes were amplified by specific primers and Universal ProbeLibrary (UPL) probes (Roche) (Table 2). Amplification efficiency based on standard curves was used to calculate mRNA concentrations. *TBP* and *IPO8* [33] were chosen as reference genes based on their stable expression in biopsies and primary culture, respectively, and because they showed similar expression levels as the target genes.

2.8. Microarray Analysis

The Illumina microarray analyses were performed as described previously [27]. Briefly, 300 ng of total RNA from each sample was reversely transcribed, amplified and Biotin-16-UTP–labeled. NanoDrop spectrophotometer and Agilent 2100 Bioanalyzer were used to measure amount (15–52 mg) and quality of the labeled cRNA. 750 ng of biotin-labeled cRNA was hybridized to the HumanRef-8v.3 (whole tissue) or HumanHT-12v.3 Illumina Sentrix BeadChip according to manufacturer's instructions. The Affymetrix microarray data from Cohort 3 were analyzed as described in detail previously [29].

2.9. RNA Sequencing

cDNA libraries were generated via the TruSeq Stranded mRNA Library Prep kit. RNA-seq was then performed at the Illumina Hiseq 4000 platform at the Genomics Core Facility, Bergen. Aligned reads were put into featureCounts (Version 1.5.2) with options "featureCounts -T 64 -p -t exon -g gene_id", resulting in a matrix of raw counts. Data were normalized and differential expression analysis was performed with DESeq2 (Version 1.22.2). For pathway enrichment analysis we used the KEGG database. Significant ontologies were visualized using ggplot2 package (Version 3.1.0). PCA plots were generated using the R package 'DESeq2' (Version 1.22.2) and the Volcano plot of the differential expression analysis by the R package 'Enhanced Volcano' (Version: 1.0.1).

2.10. Lipolysis in In Vitro Differentiated Adipocytes

Glycerol in conditioned media was measured using Free Glycerol Reagent (Sigma Aldrich) and Amplex UltraRed (Invitrogen) according to the manufacturer's instructions. Amplex Ultra Red was diluted 100-fold in Free Glycerol Reagent, mixed with 20 μL of conditioned medium in a 96-well plate, incubated at room temperature for 15 min, and fluorescence was measured (excitation/emission 530/590) using an Infinite M200 plate reader (Tecan Group, Männedorf, Switzerland). The cells were lyzed in RIPA buffer (50 mM Tris-HCl, pH 7.4, 150 mM NaCl, 0.25% deoxycholic acid, 1% NP-40, 1 mM EDTA) and protein concentration was assessed using BCA Protein Assay Kit (Thermo Fisher Scientific). Glycerol values were normalized to the proteins in each well.

2.11. SDS-PAGE and Immunoblotting

Fully differentiated SGBS cells (day 15) were transfected with 25 nM non-targeting or *RND3*-targeting siRNA for 72 h, and treated with 10 μM

Table 2
Primers and Universal ProbeLibrary (UPL) probes used for qPCR.

Gene name	Organism	Primer sequence	UPL probe
RND3	Human	F: 5′-gcgctgctccatgtcttc-3′ R: 5′- gccgtgtaattctcaaacactg-3′	38
HIF1A	Human	F: 5′-ttcacttttttcaagcagtaggaatta-3′ R: 5′-aattcttcaccctgcagtaggt-3′	74
IPO8	Human	F: 5′-cggattatagtctctgaccatgtg-3′ R: 5′-tgtgtcaccatgttcttcagg-3′	11
TBP	Human	F: 5′-tgaatcttggttgtaaacttgacc-3′ R: 5′-ctcatgattaccgcagcaaa-3′	22
Rnd3	Mouse	F: 5′-gacagccagtgtgggaaaac-3′ R: 5′-tcaaacaccgtagggacgta-3′	38
Rplp0	Mouse	F: 5′-actggtctaggacccgagaag-3′ R: 5′-tcccaccttgtctccagtct-3′	9

ROCK inhibitor for the last 24 h of the transfection. Post transfection, protein samples were prepared in RIPA buffer with phosphatase (phosSTOP; Roche) and protease inhibitors (cOmplete; Roche). After centrifugation (20,000 *g*, 4°C, 15 min), the fatty supernatant was removed, and protein concentrations were assessed by Pierce™ BCA Protein Assay kit (Thermo Fisher Scientific). Denatured protein samples were analyzed by SDS-PAGE and immunoblotting using mouse anti-RND3 (1:500, Cell Signaling#3664), rabbit anti-HSL (1:750, Cell Signaling#4107), rabbit anti phosphorylated (p) HSLser660 (human ser650) (1:750, Cell Signaling#4126) or rabbit anti-ATGL (1:750, Cell Signaling#2138) antibodies.

2.12. Statistics

P-values were calculated by ANOVA and Tukey's posthoc test or *t*-test, as indicated. Correlations were calculated by Pearson's correlation. These statistics were performed in Excel for Windows 10. For the Illumina microarray analyses we used Significance Analysis of Microarrays (SAM) to identify differentially expressed genes, as described previously [27]. Details on the statistical analysis of the Affymetrix microarrays in Cohort 3 are described in [29]. For the RNA sequencing, differentially expressed genes identified by DESeq2 (Version 1.22.2) (false discovery rate (FDR) cutoff <0.1) were used as an input and Fischer's exact test was used to identify statistically over/under represented pathways (FDR cutoff <0.05).

3. Results

3.1. Up-regulation of RND3 in Obesity and Metabolic Syndrome

To examine the expression of *RND3* in adipose tissue, we first analyzed publically available transcriptome data for two strains of mice with genetically induced obesity due to leptin deficiency (ob/ob), i.e., obesity-prone C57BL/6 (B6) and the insulin resistant-prone Black and Tan BRachyury (BTBR) [34]. In comparison to other metabolic tissues, adipose tissue showed the highest *Rnd3* mRNA expression and increased levels in the obese and insulin resistant mice compared to controls after 4 weeks of feeding, and also after 10 weeks in the BTBR model (Fig. 1A). The increased expression already at 4 weeks of overfeeding in the BTBR model is consistent with a primary effect of Rnd3 on insulin resistance and consequent diabetes, since these mice are insulin resistant at all ages independent of obesity but develop severe diabetes first after 10 weeks [34]. Although showing the lowest expression, pancreatic islets expressed significantly less *Rnd3* in both

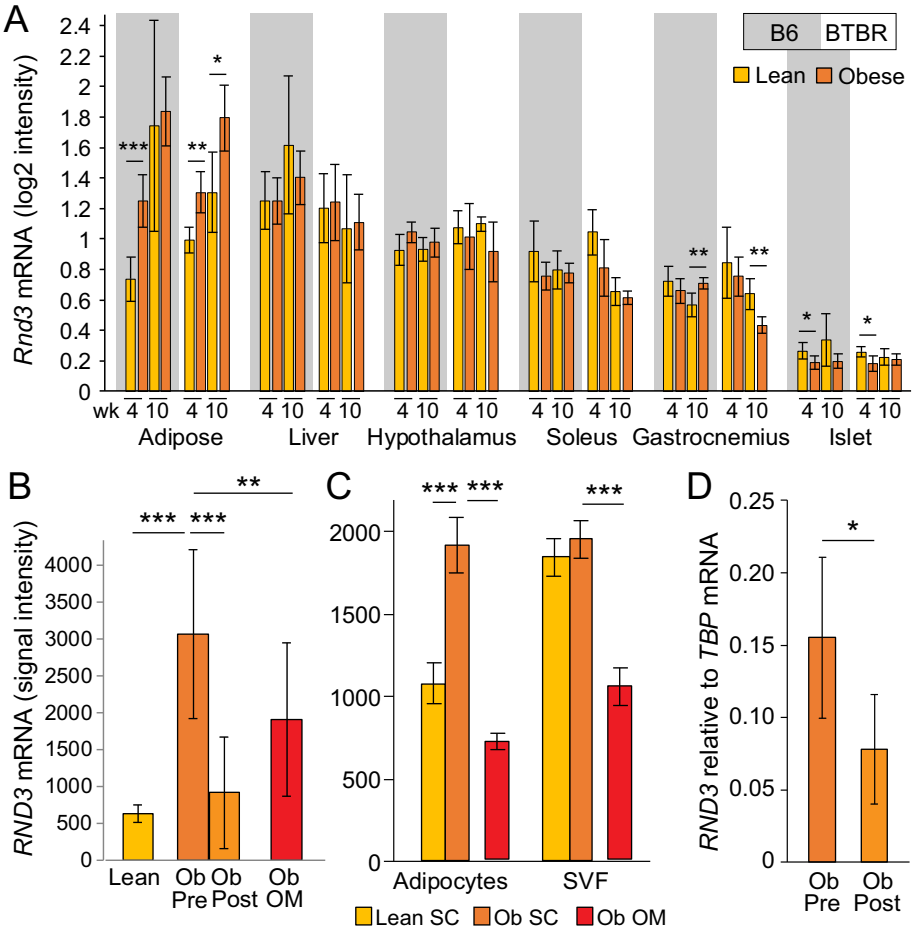

Fig. 1. Elevated adipose *RND3* mRNA expression in obesity. A. Lean and obese (ob/ob) B6 and BTBR mice were fed for 4 or 10 weeks (*ab libitum*). Adipose tissue (epididymal), liver, hypothalamus, soleus, gastrocnemius and pancreatic islets were collected ($n = 5$). Data are presented as mean ± SD. B. mRNA signal intensities were extracted from a microarray adipose transcriptome dataset (Illumina BeadChips, Cohort 1). Data are presented as mean ± SD (lean $n = 13$, subcutaneous adipose tissue obese $n = 16$, subcutaneous post-surgery $n = 16$, omental obese $n = 12$). C. Adipocytes and stromal vascular fraction (SVF) were isolated by digesting fresh human adipose tissue with collagenase. mRNA signal intensities were extracted from a microarray transcriptome dataset (Illumina BeadChips). Data are presented as mean ± SD ($n = 12$ per group). D. For a subset of the patients, adipocytes were isolated from subcutaneous adipose tissue also after profound fat loss (one year after bariatric surgery). *RND3* mRNA was measured by qPCR and related to *TBP* mRNA (reference gene). Data are presented as mean ± SD ($n = 6$). *P*-values were calculated by one-way ANOVA and Tukey's posthoc test, except panel D (paired *t*-test). B6, C57BL/6 inbred mouse strain; BTBR, Black and Tan BRachyury mouse strain; Ob, obese; Ob/ob, obese leptin-deficient; OM, omental adipose tissue; Pre, before bariatric surgery; Post, one year after bariatric surgery; SC, subcutaneous adipose tissue; SVF, stromal vascular fraction. * $p < .05$; ** $p < .01$; *** $p < .001$.

strains at 4 weeks. On the other hand, muscle (gastrocnemius) showed opposite effects in the two strains after 10 weeks (Fig. 1A).

We further compared *RND3* mRNA expression in whole adipose tissue biopsies from 13 lean and 16 extremely obese insulin resistant or diabetic Caucasians (Cohort 1, Table 1) [27]. Relative to lean samples, obese samples showed a 6-fold increase in *RND3* mRNA in abdominal subcutaneous fat, and a return to normal levels after profound fat loss due to bariatric surgery (average BMI of 33 one year after surgery) (Fig. 1B). *RND3* also showed a notable expression in omental adipose tissue from the same extremely obese patients, around 35% lower than in subcutaneous fat (Fig. 1B). In comparison, adipose expression levels of *RND1* and *RND2* were around 10-fold lower than those of RND3, and showed no alterations in obesity (Fig. S1A).

Because adipose tissue harbors a heterogeneous population of cells, including adipocytes, progenitor cells and immune cells, we measured *RND3* mRNA expression separately in adipocytes and stromal vascular fraction (SVF) isolated directly from subcutaneous (lean and obese) and omental (obese) adipose tissue ($n = 12$ in the lean and obese groups, Cohort 2, Table 1). *RND3* mRNA was expressed ~2-fold higher in isolated adipocytes from obese compared to lean samples, while we observed no such obesity-dependent expression in SVF (Fig. 1C). Consistent with the whole tissue data, omental adipocytes and SVF from the obese patients showed 40–60% lower *RND3* expression than subcutaneous adipocytes collected from the same patients (Fig. 1C). We also measured changes in *RND3* mRNA in isolated subcutaneous adipocytes collected from a subset of these patients before and after profound fat loss, and found that adipocyte *RND3* mRNA was halved (Fig. 1D), completely reversing the 2-fold higher level seen in obesity relative to lean patients (Fig. 1C).

We further examined whether *RND3* expression in isolated adipocytes might relate to whole-body insulin sensitivity and circulating lipids. We first correlated subcutaneous *RND3* mRNA across the lean and obese patients with HOMA2-IR and TAG/HDL ratio. Whereas SVF expression of *RND3* mRNA showed no correlations with these surrogate measures of insulin resistance (not shown), adipocyte *RND3* mRNA showed a strong positive correlation with both HOMA2-IR and TAG/HDL ratio (Fig. 2A). We observed a similar pattern in isolated omental adipocytes (Fig. 2A). Another cohort of 56 Caucasians (Cohort 3, Table 1) confirmed significant positive correlations for *RND3* mRNA in subcutaneous whole tissue with BMI and HOMA2-IR ($r = 0.33$, $p = .012$) (Fig. 2B), as well as with waist-to-hip ratio (WHR) ($r = 0.29$, $p = .034$) (not shown). Moreover, consistent with the relationship of adipose *RND3* with phenotypes related to insulin resistance, *RND3* correlated inversely with plasma glucose disappearance rate (KITT based on an insulin tolerance test) ($r = -0.39$, $p = .027$) (not shown).

To assess whether adipose *RND3* might contribute to these metabolic phenotypes via adipocytes, we correlated *RND3* mRNA with subcutaneous adipocyte morphology (number and size). While *RND3* showed no significant correlation with adipocyte number, we observed a strong positive correlation with subcutaneous adipocyte volume ($r = 0.47$, $p = .0002$) (Fig. 2B), and with hypertrophic fat cell morphology defined by the morphology value, i.e. the relative level of adipocyte hypertrophy or hyperplasia at any given body fat mass [35] ($r = 0.3$, $p = .02$). By multiple regression analysis we found that the positive association with adipocyte size remained significant after correcting for BMI ($\beta = 0.19$, $p = .047$), despite a strong correlation between *RND3* and BMI ($\beta = 0.67$, $p < .0001$). None of the other variables showed a significant correlation with *RND3* mRNA after BMI adjustment.

3.2. Adipose RND3 is Co-expressed with Pro-inflammatory Genes

The strong relationship between *RND3* expression and obesity-related metabolic features prompted us to explore functional roles of *RND3* in adipose tissue. To this end, we first performed co-expression analyses to predict cellular processes associated with altered *RND3* expression in vivo, for subcutaneous and omental whole adipose tissue (Cohort 1) and isolated adipocytes (Cohort 2) from patients with morbid obesity. Genes positively co-expressed with *RND3* consistently showed a significant enrichment in cellular pathways related to infection/inflammation and insulin signaling/resistance (Fig. 3A). The infection-related pathways essentially represented inflammatory genes, such as *IL6*, *TNFRSF1A*, and *NFKB*. IL17 signaling has recently

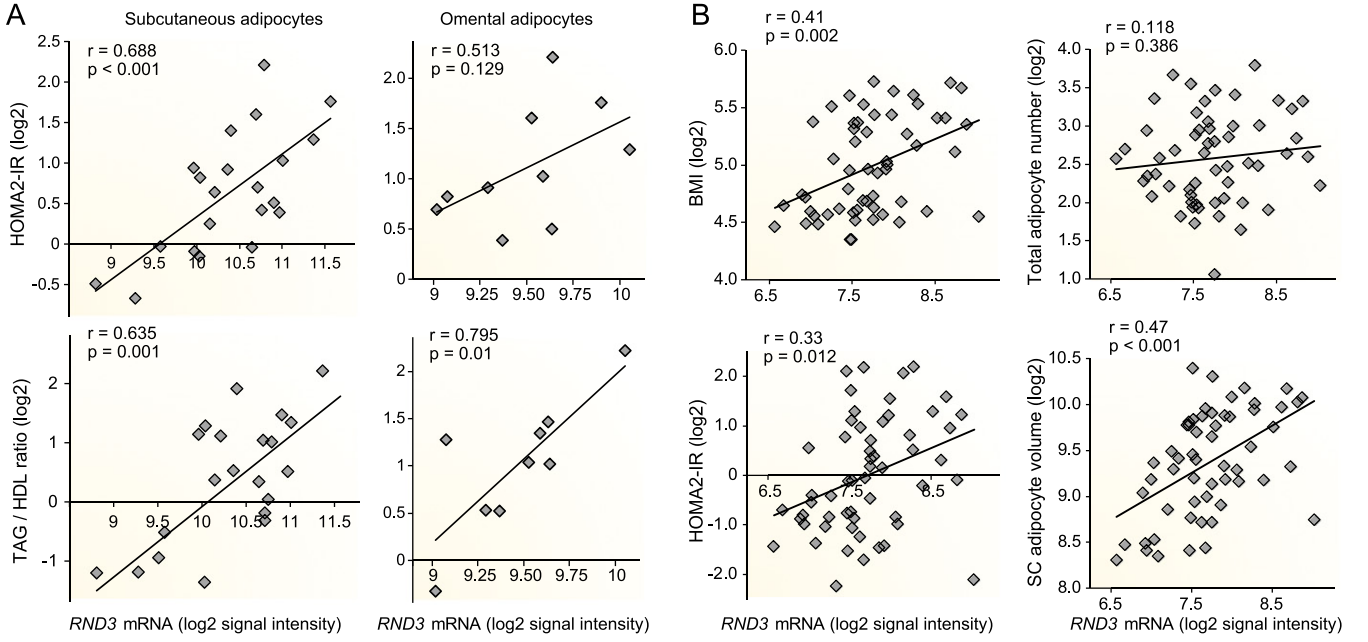

Fig. 2. Adipose RND3 mRNA correlates with insulin resistance and adipocyte size. A. *RND3* mRNA was measured by microarrays (Illumina BeadChips) in subcutaneous and omental adipocytes and correlated with HOMA2-IR and TAG/HDL ratio (Cohort 2). B. *RND3* mRNA was measured in subcutaneous adipose tissue by Affymetrix microarrays and correlated with BMI, HOMA2-IR and adipocyte number and size (Cohort 3). The Pearson correlation coefficient and *p*-value are shown. Clinical data were missing for some patients in Cohort 2. BMI, body-mass index; HDL, high-density lipoprotein cholesterol; HOMA2-IR, homeostatic model assessment 2 of insulin resistance; SC, subcutaneous; TAG, triacylglycerol.

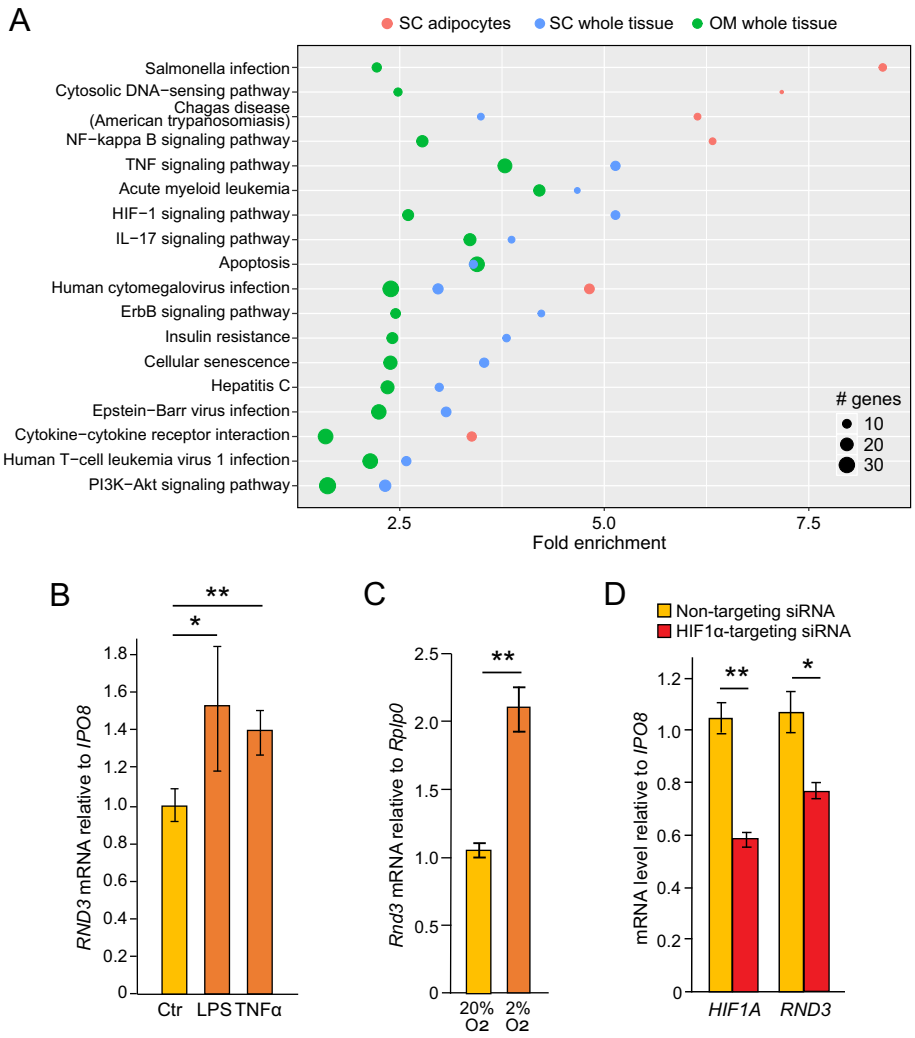

Fig. 3. Genome-wide co-expression analysis links *RND3* to inflammation and insulin resistance pathways in adipocytes. A. *RND3* mRNA levels in isolated subcutaneous adipocytes (Cohort 2) and subcutaneous or omental whole adipose tissue (Cohort 1) was correlated with other transcript levels globally (Illumina microarray analysis, log2-transformed signal intensities). Genes positively co-expressed with *RND3* (Pearson's $r \geq 0.7$) were subjected to KEGG pathway analysis (no significant KEGG pathways were retrieved for genes anti-expressed with *RND3*). Pathways with significant *RND3*-correlated gene enrichment in at least two of the three datasets are shown, sorted by enrichment in isolated adipocytes. For panels B-D, *RND3*/*Rnd3* mRNA levels were measured by qPCR, calculated relative to *IPO8* (human) or *Rplp0* (mouse), and normalized to the median value of the control triplicate in each experiment. B. Primary human adipose stromal cells (hASCs) were cultured in 24-well plates and differentiated for 3 days before stimulation with LPS (1 μg/ml) or TNFα (10 ng/ml). The data are presented as mean ± SEM for two combined experiments on adipose cells from individual subjects performed in triplicates (n = 6). C. 3 T3-L1 adipocytes were differentiated in vitro for 8 days and incubated at an atmosphere with 20% or 2% oxygen for 24 h. The data are presented as mean ± SD ($n = 3$). D. Primary hASCs were differentiated for 11 days before transfection with non-targeting (NT) siRNA or siRNA against *HIF1A* (25 nM siRNA). Cells were harvested 72 h later (day 14). The data are presented as mean ± SEM (n = 3). OM, omental; SC, subcutaneous; siRNA, small interfering RNA. * $p < .05$; ** $p < .01$.

been implicated in chronic inflammation in adipose tissue [36], in part dependent on signals from adipocytes [37]. The cytosolic DNA-sensing pathway also relates to inflammation, involving conversion of GTP and ATP to cyclic GMP-AMP (cGAMP) via cGAMP synthase (cGAS) which promotes cellular senescence via interferon signaling and inflammatory gene expression [38]. The co-expression analyses also indicated a link to HIF-1 signaling, which mediates effects of adipocyte oxygen consumption on inflammation and insulin resistance [39]. No significant enrichment was seen for the isolated omental adipocytes, nor for *RND3* anti-expressed genes regardless of sample type.

The co-expression with inflammation-related genes raised the possibility that a pro-inflammatory milieu in adipose tissue may contribute to increased *RND3* expression in obesity. To test this, we treated developing primary human adipocytes with the endotoxin lipopolysaccharide (LPS) or the cytokine tumor necrosis factor (TNF)-alpha, and found that these pro-inflammatory stimuli increased *RND3* mRNA 1.5-fold (Fig. 3B). Similarly, consistent with the co-expression of *RND3* with the HIF-1 signaling pathway, exposure of 3 T3-L1 adipocytes to hypoxia (2% O2) increased *Rnd3* mRNA 2-fold (Fig. 3C). Conversely, in differentiating primary human adipocytes, knockdown of *HIF1A* caused a 30% reduction in *RND3* expression (Fig. 3D). These data are in line with the previously reported HIF-1α-mediated transactivation of *RND3* in gastric cancer cells [26].

3.3. RND3 Knockdown Affects Metabolic and Inflammatory Genes

So far the presented data are correlative in terms of downstream functions of RND3 in adipose tissue. To establish causality, we differentiated primary human adipocytes in vitro (Fig. 4A) and performed RNA sequencing with and without siRNA-mediated knockdown of *RND3*. Based on the expression profile of *PPARG2*, a master regulator of adipogenesis and adipocyte function, we performed the knockdown on day 6–8 of differentiation coinciding with peak *PPARG2* levels on day 8 (Fig. 4B). Of note, *RND3* mRNA was largely unaltered during

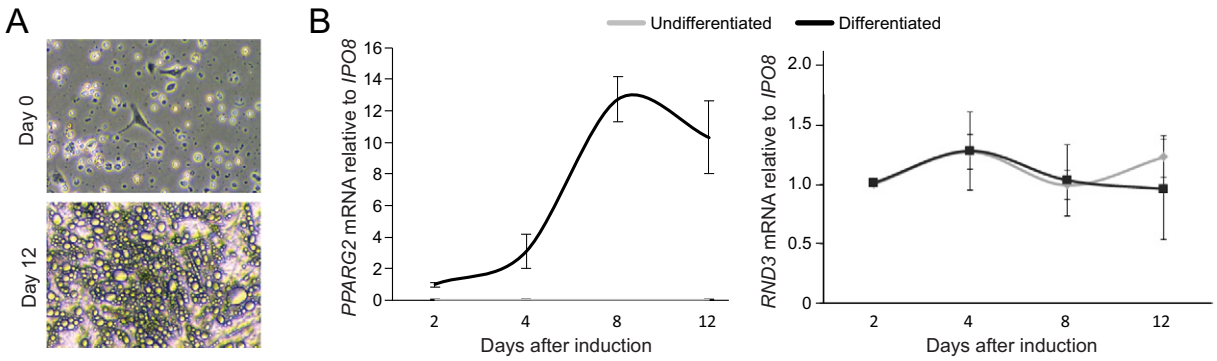

Fig. 4. Expression of *RND3* mRNA during adipogenic differentiation of primary human adipose stromal cells (hASCs). The cells were induced to differentiate by supplementing the culture medium with cortisol (100 nM/L), insulin (66 nM/L), transferrin (10 μg/mL), biotin (33 μM/L), pantothenate (17 μM/L), T3 (1 nM/L) and rosiglitazone (10 μM/L), changing medium every 2–3 days. Rosiglitazone (10 μM) was added during the first six days. A. *RND3* and *PPARG2* mRNA expression was calculated relative to IPO8 for differentiated cells and undifferentiated controls for each time-point. Data are presented as mean ± SD for independent experiments from 4 people. B. The increase in lipid accumulation as observed under the microscope (40×).

differentiation, indicating a relatively high expression in both adipocyte progenitors and mature adipocytes (qPCR Ct values around 25–26) (Fig. 4B). For primary adipocyte cultures obtained from 6 women (BMI 28.6 ± 2.4 kg/m2, age 39.5 ± 12.6 years), principal component analysis (PCA) of the RNA sequencing data showed a clear separation of samples treated with non-targeting or *RND3*-targeting siRNA (Fig. 5A). A volcano plot showed that *RND3* was, except for *DDAH1*, the most significant differentially expressed gene in cells with *RND3* knockdown, and revealed a tendency of greater overall downregulation than upregulation (Fig. 5B). Although the 6 experiments showed a notable individual variation (Fig. 5C), paired analysis of controls compared to knockdown for each individual retrieved a total of 134 downregulated and 92 upregulated genes within a false discovery rate (FDR) < 0.1 cutoff (Table S1).

Pathway analysis for these transcripts showed an enrichment of upregulated genes in adipocyte lipolysis, AMPK signaling and insulin signaling, and of downregulated genes in pro-inflammatory pathways reminiscent of the in vivo co-expression analysis (Fig. 5D). Among the genes involved in lipolysis were *ADCY1*, *IRS2*, *LIPE* and *SCD*, which were also linked to insulin-mediated suppression of lipolysis and AMPK signaling (Fig. 5E). Additional genes related to insulin signaling included *FASN*, *ACACB* and *PCK1* associated with lipid storage (e.g., *PCK1 (PEPCK)* controls adipocyte glyceroneogenesis to promote intracellular esterification of FFA to glycerol [40]).

3.4. ROCK Expression Associates with Adipocyte Metabolism and Obesity

Given the role of Rho kinase (ROCK) in mediating cellular effects of RND3, with important metabolic roles in skeletal muscle [23] and adipose tissue [41,42], we further reanalyzed a published global gene expression dataset for a mouse dedifferentiated fat (DFAT) cell line treated for 4 days with and without ROCK inhibitor [43]. Significantly enriched pathways in the ROCK-inhibitor treated cells were regulation of lipolysis in adipocytes and glycerolipid metabolism (i.e., glyceride/FFA cycling [44]), along with PPAR signaling (all for upregulated genes; no enrichment was seen for downregulated genes) (Fig. 6A). The increased expression of genes in these pathways coincided with a stimulatory effect of the ROCK inhibitor on adipogenic redifferentiation in the DFAT cells [43].

Metabolic effects of the ROCK inhibitor could depend on ROCK isoform expression. To assess the relevance of the respective isoforms in adipose and other tissues, we examined *Rock1* and *Rock2* mRNA expression levels and their changes in metabolic tissues during diet-induced obesity and insulin resistance. *Rock1* showed the highest expression in pancreatic islets, adipose tissue and liver, and *Rock2* in muscle and adipose tissue (Fig. 6B). However, only adipose tissue showed significant increases in *Rock1* as well as *Rock2* mRNA in the obese ob/ob B6 and insulin resistant BTRB mice, particularly after 4 weeks of feeding. On the other hand, liver and muscle showed significant reductions in *Rock1* mRNA, and no changes in *Rock2* mRNA (Fig. 6B).

3.5. RND3 Regulates Adipocyte Lipolysis

The effect of *RND3* knockdown on genes involved in adipocyte lipolysis prompted us to measure glycerol release as a direct measure of lipolysis. Lipolysis can be induced through increased levels of beta-adrenergic receptor activation and cAMP, with consequent activation of PKA which phosphorylates specific residues on HSL [12,13]. When treating developing primary human adipocytes with cell membrane-permeable cAMP analogs, we observed a 1.5-fold increase in *RND3* mRNA. This effect likely occurred through the PKA pathway since the cAMP analog 8CPT-cAMP, which targets PKA as well as the alternative Epac pathway, showed no additional effect compared to the PKA-specific analog 6 MB-cAMP (Fig. 7A).

We next assayed lipolysis measured as glycerol release following *RND3* knockdown in primary human adipocytes. Knockdown decreased lipolysis up to 35% depending on the cellular condition (Fig. 7B). Whereas knockdown reduced basal lipolysis only slightly, the knockdown potently attenuated cAMP-stimulated lipolysis. Conversely, treatment with ROCK inhibitor increased lipolysis about 2-fold, consistent with a positive effect of ROCK on insulin-mediated suppression of lipolysis. Surprisingly, however, the ROCK inhibitor attenuated the cAMP-stimulated lipolysis (Fig. 7B), possibly due to a saturation effect as cAMP stimulation already increased lipolysis 50-fold. We further found that RND3 knockdown inhibited lipolysis induced by isoproterenol, a catecholamine-mimicking beta3-adrenergic receptor agonist that activates cAMP/PKA signaling in adipocytes. When treated with ROCK inhibitor, to "rescue" the loss of ROCK inhibition upon RND3 knockdown, the adipocytes showed increased basal as well as isoproterenol-stimulated lipolysis as expected (Fig. 7B).

PKA-mediated phosphorylation of ser650 on HSL (typically referred to as ser660 which is the equivalent residue in rat) is an important mechanism for inducing adipocyte lipolysis in vivo, through a crosstalk with AMPK signaling which also regulates ATGL activity [14]. We therefore measured the effect of *RND3* knockdown and ROCK inhibitor on pHSLser650 by Western blotting, as well as on total HSL and ATGL levels. The Western blots confirmed a reduction in RND3 protein (Fig. 7C). Both knockdown and ROCK inhibitor reduced ATGL protein levels. Further, while total HSL levels were unchanged, levels of pHSLser650 were reduced (Fig. 7C), indicating that RND3 and RhoA/ROCK are required for PKA-mediated activation of lipolysis in adipocytes. Taken together, our clinical and experimental data support a

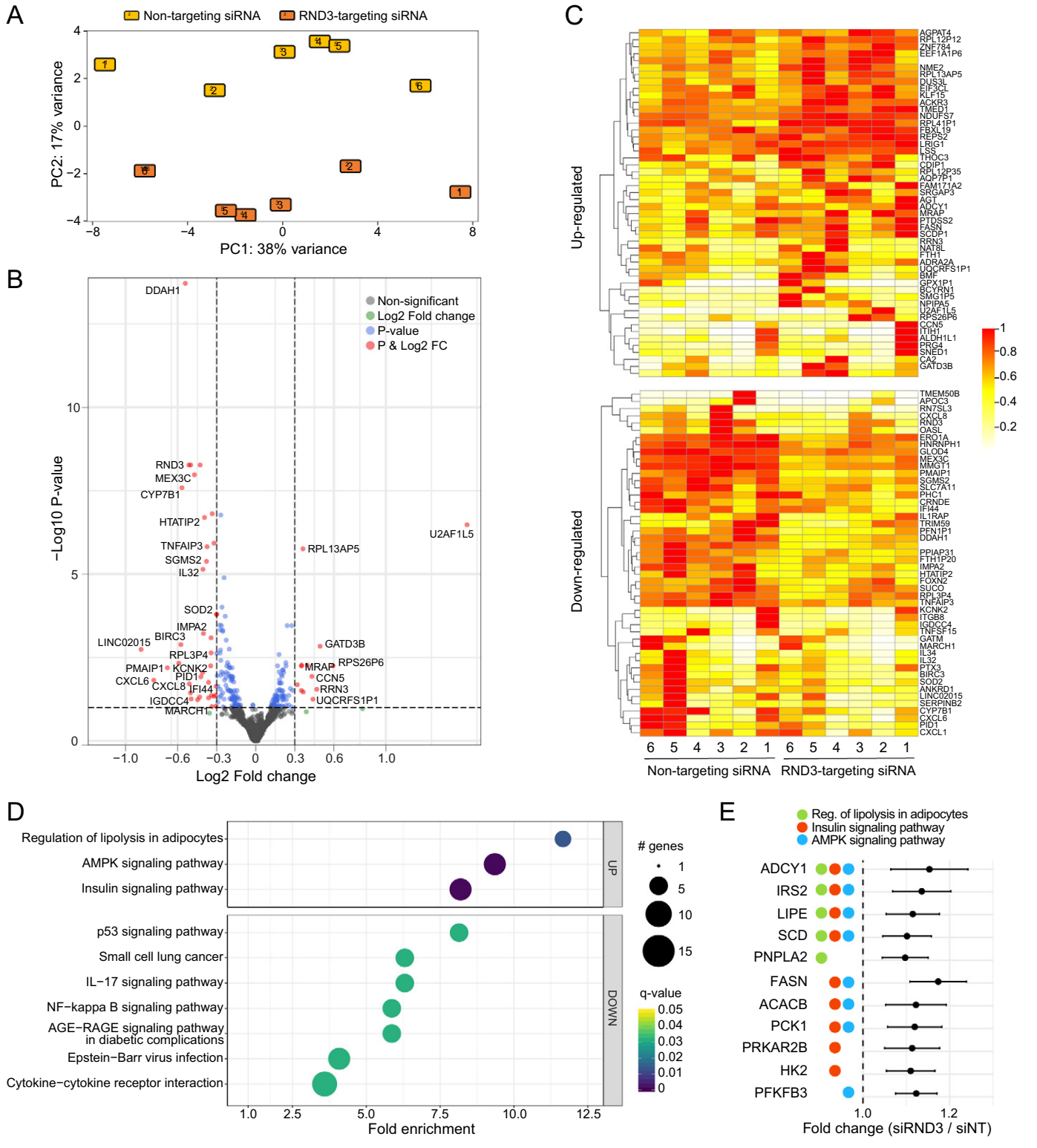

Fig. 5. *RND3* knockdown affects genes involved in lipid metabolism and inflammation in primary human adipocyte cultures. Cultures from 6 people were transfected with control non-targeting siRNA (siNT) or siRNA targeting *RND3* from day 6 to 8 after induction of adipocyte differentiation (48 h). Global gene expression was measured by RNA sequencing A. Principal component analysis (PCA) depicting the effect of *RND3* knockdown on global gene expression (adjusted for effects of the individuals). B. Volcano plot depicting fold changes for differentially expressed genes comparing non-targeting and *RND3* siRNA. C. Heatmap showing relative expression of the 50 most up-regulated and 50 most down-regulated genes with *RND3* knockdown (for genes with P.adjust <0.1 in the RNA-seq dataset). 0 represents an expression of 0, and 1 represents the maximum observed expression for that gene across all samples, to which all other samples for the same row are compared. D. KEGG pathways with a significant enrichment of differentially expressed genes with *RND3* knockdown (for genes with false discovery rate (FDR) < 0.1). All pathways passed FDR < 0.05 for enrichment. E. Relative expression of the genes in the enriched KEGG pathways for up-regulated genes with *RND3* knockdown. Data are presented as mean ± SD. Reg., Regulation; siNT, small interfering non-targeting RNA.

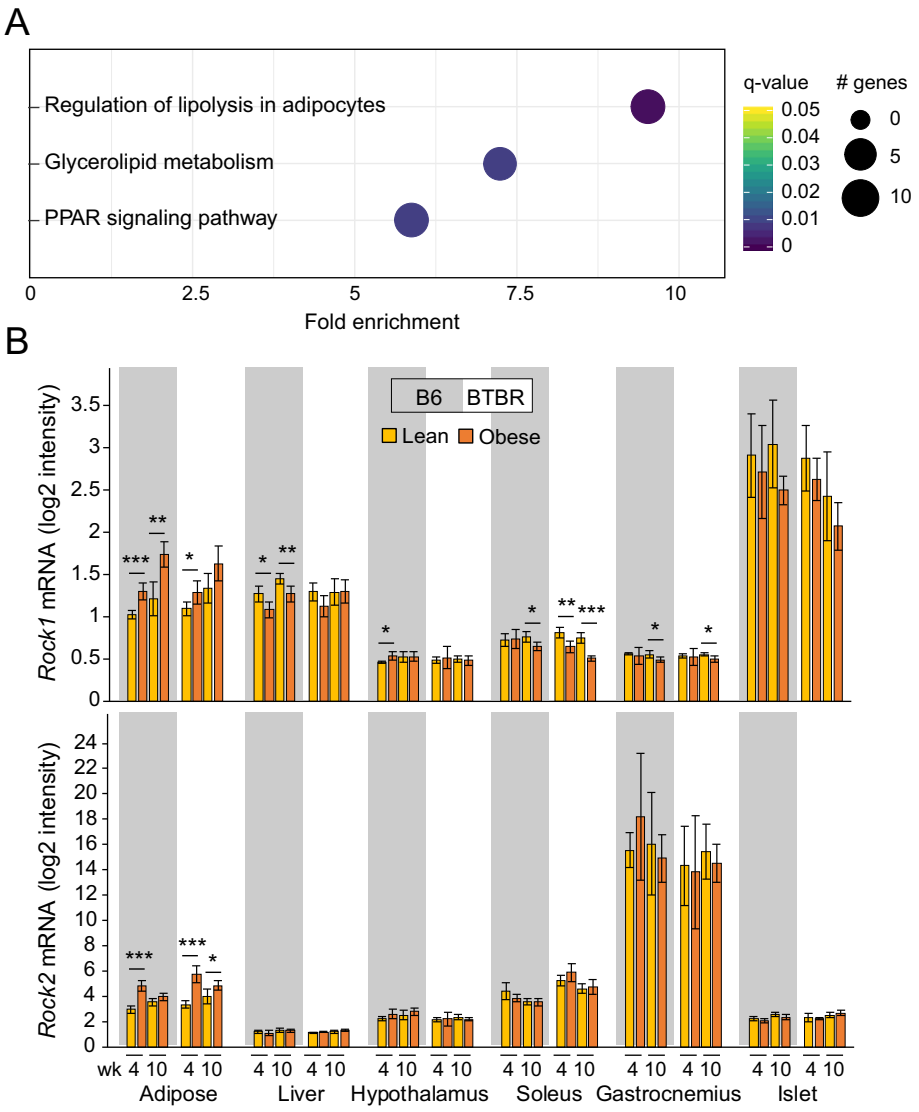

Fig. 6. Effect of ROCK inhibition on metabolic pathways in DFAT cells and expression of ROCK isoforms in tissues from obesity- and insulin resistance-prone mice. A. The mouse DFAT (dedifferentiated fat) cell line was treated for 4 days with and without ROCK inhibitor (Y-27632, 30 mM), as described previously [43]. Genes with a fold change >2 compared to control were subjected to KEGG pathway analysis, revealing highly significant fold enrichment of these genes in three categories relative to the count of genes in these pathways expected by chance. B. Lean and obese (ob/ob) B6 and BTBR mice were fed for 4 or 10 weeks (*ab libitum*). Adipose tissue (epididymal), liver, hypothalamus, soleus, gastrocnemius and pancreatic islets were analyzed (n = 5). Data are presented as mean ± SD. P-values were calculated by one-way ANOVA and Tukey's posthoc test. B6, C57BL/6 inbred mouse strain; BTBR, Black and Tan BRachyury mouse strain; Ob, obese; Ob/ob, obese leptin-deficient. * $p < .05$; ** $p < .01$; *** $p < .001$.

novel mechanism by which *RND3* promotes insulin resistance syndrome through inhibition of ROCK proteins, which alleviates an inhibitory effect on adipocyte lipolysis (Fig. 7D).

4. Discussion

In the present study we explored the potential roles of the Rho GTPase RND3 in obesity-related adipose tissue function. We revealed elevated *RND3* mRNA expression in obesity, and novel correlations between adipose *RND3* mRNA expression and features of insulin resistance syndrome in humans, including positive correlations with HOMA2-IR, TAG/HDL ratio and adipocyte size. These correlations were partly independent of BMI. Our experimental data further indicate that altered *RND3* expression causally regulates adipose tissue function, with a particular link to pathways involved in inflammatory responses and adipocyte lipid handling.

We found that RND3 knockdown consistently reduced adipocyte lipolysis, in the basal state as well as upon stimulation of lipolysis by cAMP or beta-adrenergic receptor agonist (isoproterenol). Conversely, pharmacologic inhibition of ROCK overall increased lipolysis, consistent with a lipolytic effect of RND3-mediated ROCK inhibition which may impair insulin signaling. These data are in line with our observed association between *RND3* mRNA and insulin resistance, as well as with previous studies implicating reduced skeletal muscle ROCK1 activity in systemic insulin resistance [23,45]. Further consistent with our data linking RND3 to impaired insulin signaling and lipolysis, selective inhibition of ROCK2 in 3T3-L1 adipocytes was recently shown to impair adipogenesis [42]. Furthermore, this ROCK2 inhibitor was found to promote lipid accumulation in adipose tissue macrophages (ATMs) and thereby favor macrophage polarization towards the pro-inflammatory M1 rather than the anti-inflammatory M2 type [46]. Thus, increased adipocyte lipolysis due to increased RND3 activity might promote pro-inflammatory lipid accumulation in ATMs. This effect may be further exacerbated by increased *RND3* mRNA expression upon pro-inflammatory stimuli (LPS, TNFα) as we observed in primary human hASCs. These stimuli upregulate lipolytic genes partially via

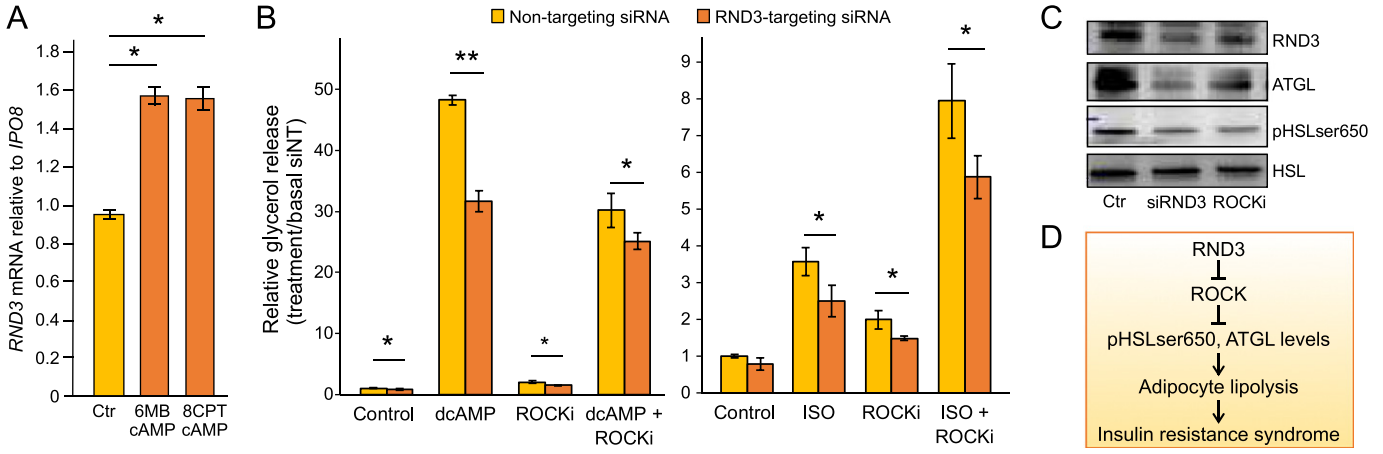

Fig. 7. Knockdown of *RND3* reduces cAMP- and isoproterenol-stimulated lipolysis. Primary human adipose stromal cells or SGBS cells were differentiated in vitro. A. Human adipose stromal cells differentiated towards adipocytes for 3 days were treated with cAMP analogs (6 MB-cAMP or 8CPT-cAMP) for 24 h. *RND3* mRNA was measured by qPCR (calculated relative to *IPO8*). Data are presented as mean ± SD. B. hASCs were transfected at day 8 of differentiation with siRNAs targeting RND3. On the day of analysis, the cells were incubated for 3 h in DMEM-F:12 medium supplemented with 20 g/L of BSA and 1 mM of dibutyryl cAMP (dcAMP) or 1 μM norepinephrine, with and without 10 μM ROCK inhibitor (ROCKi). Results are based on three individual experiments with each condition performed at least in triplicates. C. Differentiated SGBS cells (day 15) were transfected with control or RND3 siRNA for 72 h, and treated with 10 μM ROCK inhibitor for 24 h. Protein samples were analyzed by SDS-PAGE and immunoblotting (20 μg protein for the RND3 blot and 35 μg protein for the p-ser650 HSL and ATGL blots). Membranes were blocked by 5% BSA for 1 h at room temperature, followed by repeated washing in 1xTBS tween, overnight exposure to the primary antibody in buffer with 5% BSA at 4°C, repeated washing, exposure to the secondary antibody (anti-rabbit 1:10000 or anti-mouse 1:5000) in 5% BSA for 30 min at room temperature, repeated washing, and detection by ChemiDOC MP imager (BioRad). D. Proposed mechanistic model for the contribution of RND3 to insulin resistance syndrome, mediated via inhibition of ROCK signaling, supported expression and activation of rate-limiting lipolytic enzymes HSL and ATGL, and resultant augmentation of lipolysis in adipocytes. cAMP, cyclic adenosine monophosphate; ROCKi, ROCK inhibitor; siRNA, small interfering RNA. * $p < .05$; ** $p < .01$.

NFκB transcriptional activity [47] as well as cAMP [48,49]. Adipocyte RND3 may therefore be part of a vicious cycle of insulin resistance, inflammation and adipocyte lipolysis that manifests upon chronic overfeeding.

The comparison of *ROCK* expression across tissues points to an important role for both ROCK isoforms in adipose tissue, which showed increased expression in mouse models of diet-induced obesity and insulin resistance. Despite higher expression of *Rock2* in leg muscle, we only observed altered *Rock2* expression in adipose tissue. Furthermore, the change in *Rock1* expression was opposite in adipose tissue compared to other metabolic tissues. These data support specific roles for the ROCK proteins in adipocytes. The increase in ROCK expression specifically in adipose tissue might reflect a transcriptional feedback mechanism that attenuates the loss of ROCK activity upon increasing insulin resistance. It should be noted, however, that when knocking out the ROCK1 isoform selectively in adipocytes, Lee et al. found enhanced signaling through the insulin receptor, although the isoform-specific loss of ROCK1 only modestly affected whole-body insulin sensitivity [41]. It could be that the increased adipocyte lipolysis observed upon RND3 knockdown and ROCK inhibition involved enhanced insulin signaling, given the co-expression we observed upon RND3 knockdown of genes involved in lipolysis and insulin signaling, and since prolonged insulin exposure has been found to enhance cAMP- and isoproterenol-stimulated lipolysis [50]. However, the precise mechanisms that mediate the effect of RND3 on HSL/ATGL levels and adipocyte lipolysis need to be further delineated. The RNA-sequencing data suggest that AMPK signaling, which is elevated in conditions associated with lipolysis such as fasting, could also be involved. Further, we cannot rule out effects of RND3 also independent of ROCK signaling, as in the regulation of cell cycle progression [22].

Importantly, whole-body insulin sensitivity can improve upon partial inhibition of lipolysis [6,16], supporting that RND3-mediated stimulation of lipolysis may be a causal mechanism that leads to insulin resistance, and making RND3 a potential therapeutic target to prevent the development of insulin resistance, inflammation and associated metabolic diseases. We further found a positive correlation between *RND3* mRNA and adipocyte size. Adipocyte hypertrophy is a hallmark of adipose tissue inflammation in patients with insulin resistance independent of obesity [4,51]. Moreover, adipocyte hypertrophy may cause adipose and systemic insulin resistance also in the absence of adipose inflammation [52]. Despite their increased lipid accumulation, hypertrophic adipocytes are characterized by elevated rates of lipolysis, which may contribute to increased circulating FFA concentrations, ectopic lipid accumulation, and systemic insulin resistance [9,53].

The inverse relationship we found between RND3 in adipocytes and a PPARγ-related gene signature suggests a mechanism by which *RND3* promotes insulin resistance, since adipocyte PPARγ activity promotes whole-body insulin sensitivity, epitomized by pharmacologic treatment with PPARγ-specific ligands such as rosiglitazone. Rosiglitazone-mediated PPARγ activation promotes glyceroneogenesis in subcutaneous adipocytes to favor TAG synthesis over lipolysis [54], in a subtle balance between lipid storage and release with implications for systemic insulin resistance and metabolic disease risk [9]. Accordingly, we previously demonstrated that adipocytes of people who are susceptible to insulin resistance and T2D, as a result of carrying a T2D risk allele in the *PPARG* locus, have decreased glyceroneogenesis (pyruvate incorporation into TAG) and increased lipolysis (FFA release) [55]. Consistently, dose-dependent restoration of insulin resistance with rosiglitazone involves decreased levels of cAMP and inhibition of lipolysis [56]. It should be noted that elevated circulating FFA levels in T2D may also result from de novo lipogenesis and impaired lipid handling independent of lipolysis [17].

It is further possible that RND3 at least partly affected adipocyte lipolysis by modulating actin stress fibers and cell structure, as a primary function of RND3 is to serve as an endogenous antagonist of RhoA/ROCK signaling and thereby modulate actin cytoskeleton dynamics [21]. Effects of RhoA/ROCK signaling on cytoskeleton dynamics has been implicated in adipocyte function [43]. Another small GTPase which regulates actin cytoskeleton, membrane receptor trafficking and endocytosis, ADP-ribosylation factor 6 (Arf6), has been found to modulate lipolysis in response to beta-adrenergic (but not cAMP) stimulation, which may involve adrenergic receptor trafficking [57]. In line with our findings for RND3 knockdown, Arf6 knockdown in 3 T3-L1 adipocytes reduced isoproterenol-stimulated lipolysis. Future studies should explore the possible role of altered

actin cytoskeleton and receptor trafficking in mediating the RND3-dependent regulation of lipolysis.

Our study has strengths as well as limitations. A major strength of our study is the analyses of adipose gene expression and clinical data in several human cohorts, and experimental and functional assays performed in primary human adipocyte cultures based on a systematic whole-genome screen. On the other hand, the in vivo human expression data were correlative and do not establish causality, and we cannot necessarily extrapolate the in vitro data to an organismal context. For example, although we found a causal effect of RND3 perturbation on adipocyte lipolysis in cultured primary human adipocytes, e.g., in the context of cAMP signaling which partly mediates lipolytic effects of pro-inflammatory stimuli [48,49], these cultures do not necessarily reflect the context of cellular stress associated with obesity and insulin resistance in vivo. Thus, our data encourage future studies that perturb adipocyte Rnd3 in vivo, such as by adipocyte-specific conditional knockout in a mouse model of diet-induced obesity and insulin resistance. Finally, although we used ROCK inhibitor to mimic increased endogenous RND3 activity, RND3 overexpression in primary human adipocytes could further inform on the dynamics of lipolysis regulation at different RND3 levels, also in the context of adipose tissue stress related to insulin resistance. In primary in vitro differentiated adipocytes, such studies must be carefully balanced to ensure physiological expression levels and avoid non-specific toxic effects.

5. Conclusion

In conclusion, we here uncovered a differential expression of adipose *RND3* in obesity and insulin resistance, and a causal role for RND3 in adipocyte lipolysis. Mechanistically, RND3 knockdown reduced protein levels of both ATGL and ser650-phosphorylated HSL, attenuating the stimulatory effects of isoproterenol and cAMP signaling on lipolysis. These clinical and experimental data together highlight RND3 as a novel potential target for therapeutic intervention to improve adipocyte lipid handling and ameliorate obesity-related insulin resistance.

Supplementary data to this article can be found online at https://doi.org/10.1016/j.metabol.2019.153999.

Author Contributions

TR, GM and SND conceived and designed the study and analyzed data. TR, AK, ZF and SND performed the experiments. SND, GM, JVS, TS, HH, PA, MR contributed to the collection of adipose tissue samples and data interpretation. SND wrote the manuscript, and all coauthors reviewed and approved the final version.

Acknowledgments

We thank the people who contributed samples to this study, and the surgeons who collected adipose tissue. We thank Margit Solsvik, Jan-Inge Bjune, Linn Skartveit and Alba Kaci for expert technical assistance and Laurence Dyer for bioinformatics support. This work was supported by the Western Norway Health Authority, Norway; Trond Mohn Foundation, Bergen, Norway; the Swedish Research Council, Sweden; the NovoNordisk Foundation (NNF15CC0018486 and NNF15AS0018346); CIMED, Sweden; the Swedish Diabetes Foundation, Sweden; the Stockholm County Council, Sweden; the Strategic Research Program in Diabetes at Karolinska Institutet, Sweden; Clinical Cooperation Group "Nutrigenomics and Type 2 Diabetes", Helmholtz Center Munich, Germany; and the Else Kroener-Fresenius-Foundation, Bad Homburg, Germany.

Declaration of Competing Interest

All authors declare no conflict of interest.

References

[1] The GBD 2015 Obesity Collaborators. Health effects of overweight and obesity in 195 countries over 25 years. N Engl J Med 2017;377:13–27. https://doi.org/10.1056/NEJMOA1614362.
[2] Xu H, Barnes GT, Yang Q, Tan G, Yang D, Chou CJ, et al. Chronic inflammation in fat plays a crucial role in the development of obesity-related insulin resistance. J Clin Invest 2003;112:1821–30. https://doi.org/10.1172/JCI19451.
[3] Schenk S, Saberi M, Olefsky JM. Insulin sensitivity: modulation by nutrients and inflammation. J Clin Invest 2008;118:2992–3002. https://doi.org/10.1172/JCI34260.
[4] Klöting N, Fasshauer M, Dietrich A, Kovacs P, Schön MR, Kern M, et al. Insulin-sensitive obesity. Am J Physiol Endocrinol Metab 2010;299:E506–15. https://doi.org/10.1152/ajpendo.00586.2009.
[5] Guilherme A, Virbasius JV, Puri V, Czech MP. Adipocyte dysfunctions linking obesity to insulin resistance and type 2 diabetes. Nat Rev Mol Cell Biol 2008;9:367–77. https://doi.org/10.1038/nrm2391.
[6] Girousse A, Tavernier G, Valle C, Moro C, Mejhert N, Dinel A-L, et al. Partial inhibition of adipose tissue lipolysis improves glucose metabolism and insulin sensitivity without alteration of fat mass. PLoS Biol 2013;11:e1001485. https://doi.org/10.1371/journal.pbio.1001485.
[7] Strawbridge RJ, Laumen H, Hamsten A, Breier M, Grallert H, Hauner H, et al. Effects of genetic loci associated with central obesity on adipocyte lipolysis. PLoS One 2016;11:e0153990. https://doi.org/10.1371/journal.pone.0153990.
[8] Rydén M, Arner P. Subcutaneous adipocyte lipolysis contributes to circulating lipid levels. Arterioscler Thromb Vasc Biol 2017;37:1782–7. https://doi.org/10.1161/ATVBAHA.117.309759.
[9] Saponaro C, Gaggini M, Carli F, Gastaldelli A. The subtle balance between lipolysis and Lipogenesis: a critical point in metabolic homeostasis. Nutrients 2015;7:9453–74. https://doi.org/10.3390/nu7115475.
[10] Krintel C, Mörgelin M, Logan DT, Holm C. Phosphorylation of hormone-sensitive lipase by protein kinase a in vitro promotes an increase in its hydrophobic surface area. FEBS J 2009;276:4752–62. https://doi.org/10.1111/j.1742-4658.2009.07172.x.
[11] Anthonsen MW, Rönnstrand L, Wernstedt C, Degerman E, Holm C. Identification of novel phosphorylation sites in hormone-sensitive lipase that are phosphorylated in response to isoproterenol and govern activation properties in vitro. J Biol Chem 1998;273:215–21. https://doi.org/10.1074/jbc.273.1.215.
[12] Lorente-Cebrián S, Kulyté A, Hedén P, Näslund E, Arner P, Rydén M. Relationship between site-specific HSL phosphorylation and adipocyte lipolysis in obese women. Obes Facts 2011;4:365–71. https://doi.org/10.1159/000334036.
[13] Duncan RE, Ahmadian M, Jaworski K, Sarkadi-Nagy E, Sul HS. Regulation of lipolysis in adipocytes. Annu Rev Nutr 2007;27:79–101. https://doi.org/10.1146/annurev.nutr.27.061406.093734.
[14] Kim S-J, Tang T, Abbott M, Viscarra JA, Wang Y, Sul HS. AMPK phosphorylates Desnutrin/ATGL and hormone-sensitive lipase to regulate lipolysis and fatty acid oxidation within adipose tissue. Mol Cell Biol 2016;36:1961–76. https://doi.org/10.1128/MCB.00244-16.
[15] Wiedemann MS, Wueest S, Grob A, Item F, Schoenle EJ, Konrad D. Short-term HFD does not alter lipolytic function of adipocytes. Adipocyte 2014;3:115–20. https://doi.org/10.4161/adip.27575.
[16] Morigny P, Houssier M, Mouisel E, Langin D. Adipocyte lipolysis and insulin resistance. Biochimie 2016;125:259–66. https://doi.org/10.1016/J.BIOCHI.2015.10.024.
[17] Pereira MJ, Skrtic S, Katsogiannos P, Abrahamsson N, Sidibeh CO, Dahgam S, et al. Impaired adipose tissue lipid storage, but not altered lipolysis, contributes to elevated levels of NEFA in type 2 diabetes. Degree of hyperglycemia and adiposity are important factors. Metabolism 2016;65:1768–80. https://doi.org/10.1016/j.metabol.2016.09.008.
[18] Chardin P. Function and regulation of Rnd proteins. Nat Rev Mol Cell Biol 2006;7:54–62. https://doi.org/10.1038/nrm1788.
[19] Fiegen D, Blumenstein L, Stege P, Vetter IR, Ahmadian MR. Crystal structure of Rnd3/RhoE: functional implications. FEBS Lett 2002;525:100–4. https://doi.org/10.1016/S0014-5793(02)03094-6.
[20] Foster R, Hu KQ, Lu Y, Nolan KM, Thissen J, Settleman J. Identification of a novel human rho protein with unusual properties: GTPase deficiency and in vivo farnesylation. Mol Cell Biol 1996;16:2689–99. https://doi.org/10.1128/mcb.16.6.2689.
[21] Jie W, Andrade KC, Lin X, Yang X, Yue X, Chang J. Pathophysiological functions of Rnd3/RhoE. Compr Physiol 2015;6:169–86. https://doi.org/10.1002/cphy.c150018.
[22] Riento K, Villalonga P, Garg R, Ridley A. Function and regulation of RhoE. Biochem Soc Trans 2005;33:649–51. https://doi.org/10.1042/BST0330649.
[23] Chun K-H, Choi K-D, Lee D-H, Jung Y, Henry RR, Ciaraldi TP, et al. In vivo activation of ROCK1 by insulin is impaired in skeletal muscle of humans with type 2 diabetes. Am J Physiol Endocrinol Metab 2011;300:E536–42. https://doi.org/10.1152/ajpendo.00538.2010.
[24] Regazzetti C, Peraldi P, Grémeaux T, Najem-Lendom R, Ben-Sahra I, Cormont M, et al. Hypoxia decreases insulin signaling pathways in adipocytes. Diabetes 2009;58:95–103. https://doi.org/10.2337/db08-0457.
[25] Trayhurn P. Hypoxia and adipose tissue function and dysfunction in obesity. Physiol Rev 2013;93:1–21. https://doi.org/10.1152/physrev.00017.2012.
[26] Zhou J, Li K, Gu Y, Feng B, Ren G, Zhang L, et al. Transcriptional up-regulation of RhoE by hypoxia-inducible factor (HIF)-1 promotes epithelial to mesenchymal transition of gastric cancer cells during hypoxia. Biochem Biophys Res Commun 2011;415:348–54. https://doi.org/10.1016/J.BBRC.2011.10.065.
[27] Dankel SN, Fadnes DJ, Stavrum A-K, Stansberg C, Holdhus R, Hoang T, et al. Switch from stress response to homeobox transcription factors in adipose tissue after profound fat loss. PLoS One 2010;5:e11033. https://doi.org/10.1371/journal.pone.0011033.
[28] Methlie P, Dankel S, Myhra T, Christensen B, Gjerde J, Fadnes D, et al. Changes in adipose glucocorticoid metabolism before and after bariatric surgery assessed by direct

hormone measurements. Obesity (Silver Spring) 2013;21:2495–503. https://doi.org/10.1002/oby.20449.
[29] Arner E, Mejhert N, Kulyté A, Balwierz PJ, Pachkov M, Cormont M, et al. Adipose tissue microRNAs as regulators of CCL2 production in human obesity. Diabetes 2012;61:1986–93. https://doi.org/10.2337/db11-1508.
[30] Veum VL, Dankel SN, Gjerde J, Nielsen HJ, Solsvik MH, Haugen C, et al. The nuclear receptors NUR77, NURR1 and NOR1 in obesity and during fat loss. Int J Obes (Lond) 2012;36:1195–202. https://doi.org/10.1038/ijo.2011.240.
[31] Dankel SN, Degerud EM, Borkowski K, Fjære E, Midtbø LK, Haugen C, et al. Weight cycling promotes fat gain and altered clock gene expression in adipose tissue in C57BL/6J mice. Am J Physiol Metab 2014;306:E210–24. https://doi.org/10.1152/ajpendo.00188.2013.
[32] Wabitsch M, Brenner R, Melzner I, Braun M, Möller P, Heinze E, et al. Characterization of a human preadipocyte cell strain with high capacity for adipose differentiation. Int J Obes (Lond) 2001;25:8–15. https://doi.org/10.1038/sj.ijo.0801520.
[33] Hurtado del Pozo C, Calvo RM, Vesperinas-García G, Gómez-Ambrosi J, Frühbeck G, Corripio-Sánchez R, et al. IPO8 and FBXL10: new reference genes for gene expression studies in human adipose tissue. Obesity 2010;18:897–903. https://doi.org/10.1038/oby.2009.374.
[34] Keller MP, Choi Y, Wang P, Davis DB, Rabaglia ME, Oler AT, et al. A gene expression network model of type 2 diabetes links cell cycle regulation in islets with diabetes susceptibility. Genome Res 2008;18:706–16. https://doi.org/10.1101/gr.074914.107.
[35] Eriksson-Hogling D, Andersson DP, Bäckdahl J, Hoffstedt J, Rössner S, Thorell A, et al. Adipose tissue morphology predicts improved insulin sensitivity following moderate or pronounced weight loss. Int J Obes (Lond) 2015;39:893–8. https://doi.org/10.1038/ijo.2015.18.
[36] Chehimi M, Vidal H, Eljaafari A. Pathogenic role of IL-17-producing immune cells in obesity, and related inflammatory diseases. J Clin Med 2017;6. https://doi.org/10.3390/jcm6070068.
[37] Chehimi M, Robert M, Bechwaty ME, Vial G, Rieusset J, Vidal H, et al. Adipocytes, like their progenitors, contribute to inflammation of adipose tissues through promotion of Th-17 cells and activation of monocytes, in obese subjects. Adipocyte 2016;5:275–82. https://doi.org/10.1080/21623945.2015.1134402.
[38] Li T, Chen ZJ. The cGAS–cGAMP–STING pathway connects DNA damage to inflammation, senescence, and cancer. J Exp Med 2018;215:1287–99. https://doi.org/10.1084/JEM.20180139.
[39] Lee YS, Kim J, Osborne O, Oh DY, Sasik R, Schenk S, et al. Increased adipocyte O2 consumption triggers HIF-1α, causing inflammation and insulin resistance in obesity. Cell 2014;157:1339–52. https://doi.org/10.1016/J.CELL.2014.05.012.
[40] Nye CK, Hanson RW, Kalhan SC. Glyceroneogenesis is the dominant pathway for triglyceride glycerol synthesis in vivo in the rat. J Biol Chem 2008;283:27565–74. https://doi.org/10.1074/jbc.M804393200.
[41] Lee S-H, Huang H, Choi K, Lee DH, Shi J, Liu T, et al. ROCK1 isoform-specific deletion reveals a role for diet-induced insulin resistance. Am J Physiol Endocrinol Metab 2014;306:E332–43. https://doi.org/10.1152/ajpendo.00619.2013.
[42] Diep DTV, Hong K, Khun T, Zheng M. Ul-Haq a, Jun H-S, et al. anti-adipogenic effects of KD025 (SLx-2119), a ROCK2-specific inhibitor, in 3T3-L1 cells. Sci Rep 2018;8:2477. https://doi.org/10.1038/s41598-018-20821-3.
[43] Nobusue H, Onishi N, Shimizu T, Sugihara E, Oki Y, Sumikawa Y, et al. Regulation of MKL1 via actin cytoskeleton dynamics drives adipocyte differentiation. Nat Commun 2014;5:3368. https://doi.org/10.1038/ncomms4368.
[44] Prentki M, Madiraju SRM. Glycerolipid metabolism and signaling in health and disease. Endocr Rev 2008;29:647–76. https://doi.org/10.1210/er.2008-0007.
[45] Lee DH, Shi J, Jeoung NH, Kim MS, Zabolotny JM, Lee SW, et al. Targeted disruption of ROCK1 causes insulin resistance in vivo. J Biol Chem 2009;284:11776–80. https://doi.org/10.1074/jbc.C900014200.
[46] Zandi S, Nakao S, Chun K-H, Fiorina P, Sun D, Arita R, et al. ROCK-isoform-specific polarization of macrophages associated with age-related macular degeneration. Cell Rep 2015;10:1173–86. https://doi.org/10.1016/j.celrep.2015.01.050.
[47] Laurencikiene J, van Harmelen V, Arvidsson Nordström E, Dicker A, Blomqvist L, Näslund E, et al. NF-kappaB is important for TNF-alpha-induced lipolysis in human adipocytes. J Lipid Res 2007;48:1069–77. https://doi.org/10.1194/jlr.M600471-JLR200.
[48] Zhang HH, Halbleib M, Ahmad F, Manganiello VC, Greenberg AS. Tumor necrosis factor-alpha stimulates lipolysis in differentiated human adipocytes through activation of extracellular signal-related kinase and elevation of intracellular cAMP. Diabetes 2002;51:2929–35. https://doi.org/10.2337/diabetes.51.10.2929.
[49] Grisouard J, Bouillet E, Timper K, Radimerski T, Dembinski K, Frey DM, et al. Both inflammatory and classical lipolytic pathways are involved in lipopolysaccharide-induced lipolysis in human adipocytes. Innate Immun 2012;18:25–34. https://doi.org/10.1177/1753425910386632.
[50] Botion LM, Green A. Long-term regulation of lipolysis and hormone-sensitive lipase by insulin and glucose. Diabetes 1999;48:1691–7. https://doi.org/10.2337/DIABETES.48.9.1691.
[51] Henninger AMJ, Eliasson B, Jenndahl LE, Hammarstedt A. Adipocyte hypertrophy, inflammation and fibrosis characterize subcutaneous adipose tissue of healthy, non-obese subjects predisposed to type 2 diabetes. PLoS One 2014;9. https://doi.org/10.1371/journal.pone.0105262.
[52] Kim JI, Huh JY, Sohn JH, Choe SS, Lee YS, Lim CY, et al. Lipid-overloaded enlarged adipocytes provoke insulin resistance independent of inflammation. Mol Cell Biol 2015;35:1686–99. https://doi.org/10.1128/MCB.01321-14.
[53] Acosta JR, Douagi I, Andersson DP, Bäckdahl J, Rydén M, Arner P, et al. Increased fat cell size: a major phenotype of subcutaneous white adipose tissue in non-obese individuals with type 2 diabetes. Diabetologia 2016;59:560–70. https://doi.org/10.1007/s00125-015-3810-6.
[54] Cadoudal T, Blouin JM, Collinet M, Fouque F, Tan GD, Loizon E, et al. Acute and selective regulation of glyceroneogenesis and cytosolic phosphoenolpyruvate carboxykinase in adipose tissue by thiazolidinediones in type 2 diabetes. Diabetologia 2007;50:666–75. https://doi.org/10.1007/s00125-006-0560-5.
[55] Claussnitzer M, Dankel SN, Klocke B, Grallert H, Glunk V, Berulava T, et al. Leveraging cross-species transcription factor binding site patterns: from diabetes risk loci to disease mechanisms. Cell 2014;156:343–58. https://doi.org/10.1016/j.cell.2013.10.058.
[56] He J, Xu C, Kuang J, Liu Q, Jiang H, Mo L, et al. Thiazolidinediones attenuate lipolysis and ameliorate dexamethasone-induced insulin resistance. Metabolism 2015;64:826–36. https://doi.org/10.1016/J.METABOL.2015.02.005.
[57] Liu Y, Zhou D, Abumrad NA, Su X. ADP-ribosylation factor 6 modulates adrenergic stimulated lipolysis in adipocytes. Am J Physiol Cell Physiol 2010;298:C921–8. https://doi.org/10.1152/ajpcell.00541.2009.